THE COMBINED USE OF 3D T1- AND T2-WEIGHTED SEQUENCES IMPROVES CERVICAL CORD LESION DETECTION IN PATIENTS WITH MULTIPLE SCLEROSIS: A MULTICENTER STUDY AT 3T

L. Storelli[1], M. Aboulwafa[1], M. A. Rocca[1,2], P. Valsasina[1], P. Preziosa[1], M. Copetti[1,3], A. Rovira[4], X. Montalban[4], H. Kearney[5], O. Ciccarelli[5], L. Matthews[6], J. Palace[6], A. Gallo[7], A. Bisecco[7], C. Lukas[8], B. Bellenberg[8], G. Comi[2], M. Filippi[1]

[1]Neuroimaging Research Unit, Institute of Experimental Neurology; [2]Dept. of Neurology, San Raffaele Scientific Institute, Vita-Salute San Raffaele University, Milan, Italy; [3]Biostatistic Unit, IRCCS Casa Sollievo della Sofferenza, San Giovanni Rotondo, Foggia, Italy; [4]CEM-Cat, Hospital Universitari Vall d'Hebron, Barcelona, Spain; [5]Queen Square MS Center, UCL Institute of Neurology, London, UK; [6]University of Oxford Hospitals Trust, Oxford, UK; [7]Second University of Naples and Institute of Diagnosis and Care "Hermitage-Capodimonte", Naples, Italy; [8]St Josef Hospital, Ruhr University, Bochum, Germany.

INTRODUCTION and PURPOSE

- The spinal cord is an eloquent site of the central nervous system that is frequently involved in MS.
- Cervical cord lesions are more specific for MS compared to brain lesions (Bot et al., 2002).
- Cord lesions can be found early in the course of the disease and contribute to the diagnostic process (Filippi et al., 2016).
- MR imaging of the spinal cord presents inherent difficulties that make acquisition technically challenging for spatially non-uniform magnetic field environment of the spinal cord, the small physical dimension of its cross-section, and the physiological motion related to the pulsating CSF flow, heartbeat and breathing (Stroman et al., 2014).
- In the clinical practice, cord lesions are detected on proton density or T2-weighted sagittal scans.
- The introduction of high-field scanners has shown that the use of T1-weighted high-resolution cord sequences may improve cord lesion detection (Nair et al., 2013).

In this study, we evaluated lesion visualization in the cervical cord on 3D T1-weighted scans *vs* T2-weighted (or short-tau inversion recovery) MRI acquired at 3.0 T in a large dataset of MS patients acquired at 6 European sites.

METHODS

Subjects. Patients were enrolled at six European centers part of the MAGNIMS network: Hospital Universitari Vall d'Hebron, Barcelona, (Spain); St. Josef Hospital Ruhr University Bochum (Germany); Queen Square MS Centre, UCL Institute of Neurology, London (UK); Neuroimaging Research Unit, San Raffaele Scientific Institute, Milan (Italy); University of Oxford Hospitals Trust, Oxford, (UK); the MRI Center "SUN-FISM", Second University of Naples, Naples (Italy).

Table 1 summarizes the main demographic and clinical characteristics of the patients enrolled.

	All MS	BMS	CIS	RRMS	SPMS	PPMS
Patients	203	19	32	95	37	20
Sex (F/M)	120/83	9/10	21/11	61/34	23/14	6/14
Age [y] (SD)	43.5 (12.0)	44.5 (7.7)	34 (8.8)	40.8 (11.9)	52.2 (8.8)	53.8 (8.2)
Median EDSS (range)	2.5 (0-8)	1.5 (1-3)	1.5 (0-4)	2.6 (0-6)	5.9 (3-8)	6.0 (3-8)
Disease Duration [y] (SD)	12.5 (9.5)	18.8 (3.6)	0.9 (0.58)	8.6 (7.0)	21.6 (10.6)	12.6 (5.3)

Abbreviations: BMS=benign multiple sclerosis; CIS=clinically isolated syndromes; RR=relapsing-remitting; SP=secondary progressive; PP=primary progressive; EDSS=expanded disability status scale; F=female; M=male; SD=standard deviation.

MRI Acquisition.
Cervical cord MRI scans were obtained using 3.0 Tesla scanners at all sites (Barcelona: Siemens Trio; Oxford: Siemens Prisma; Bochum, London and Milan: Philips Achieva; Naples: GE Signa).
The following cervical cord sequences were obtained: sagittal dual-echo turbo-spin-echo (TSE) (London, Oxford); sagittal short tau inversion recovery (STIR) (Barcelona, Bochum, Milan, Naples); and sagittal 3D T1-weighted magnetization-prepared rapid acquisition gradient echo (MP-RAGE) scan (all sites).

Figure 1. Intra- and inter-rater MRI analysis of cord lesions.

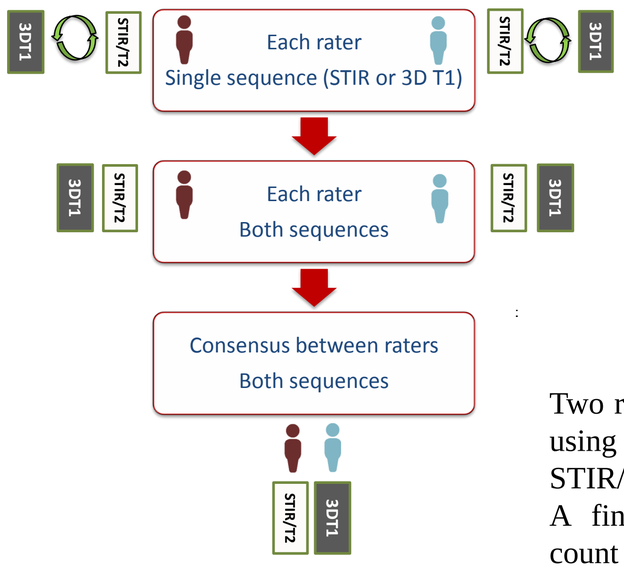

Focal Lesion Analysis:
1) lesion count (from top of C2 to the lower border of C7);
2) rating of lesion cervical level;
3) rating of the number of involved cord segments;
4) axial localization (reformatting 3DT1 into axial view using Jim 6.0 software).

Two raters, blindly, evaluated cord lesions, using STIR/DE only, 3D T1 only, and then STIR/DE and 3D T1 together.
A final consensus agreement on lesion count and location was made (**Figure 1**).

Statistical Analysis.
Inter-observer agreement on lesion number: concordance correlation coefficient (CCC) on each sequence, separately, and on the two sequences, used together.
The number of lesions detected by each rater on STIR/DE, 3D T1, separately, and on STIR/DE and 3D T1 together was compared using a t test for paired samples. Lesion counts were compared between sequences using mixed effect models with unstructured covariance matrix, adjusted for site.
Inter-sequence agreement on lesion location (expressed in terms of cervical cord level) was assessed using the Cohen's kappa index.
Correlations between lesion counts and clinical variables: Spearman's Rank correlation coefficient.

RESULTS

Inter-rater concordance on the number of detected lesions was high when using STIR/DE alone (CCC=0.888), 3D T1 alone (CCC=0.92) and the two sequences together (CCC=0.909).

Table 2. Consensus lesion count, on STIR/DE, 3D T1 and the combination of both sequences.

	All MS	BMS	CIS	RRMS	SPMS	PPMS
STIR/DE Median (range)	743 3 (0-11)	81 3 (1-11)	54 0 (0-9)	313 3 (0-11)	195 5 (1-10)	100 4 (0-11)
3D T1 Median (range)	745 3 (0-11)	70 3 (0-10)	60 0 (0-9)	299 3 (0-11)	204 6(1-10)	112 5 (1-11)
Combined lesion count (STIR/DE and 3D T1) Median (range)	835 4 (0-12)	92 4 (1-12)	65 0 (0-9)	342 3 (0-11)	222 6(1-10)	114 5 (1-11)

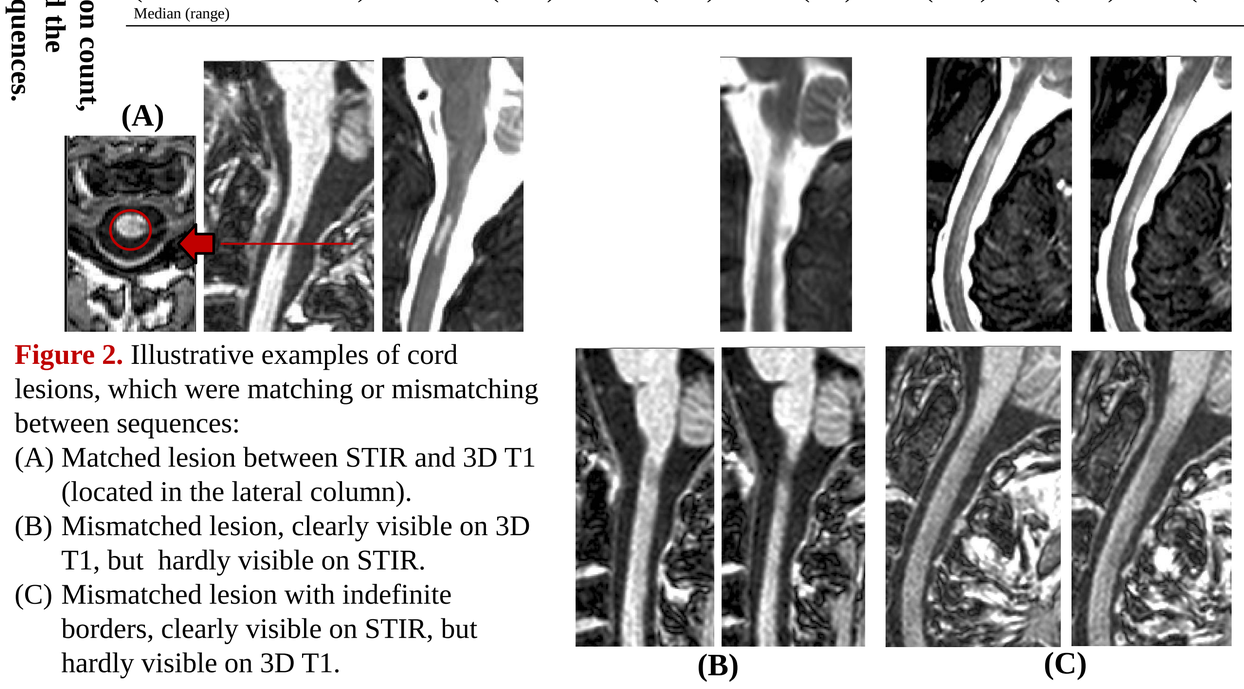

Figure 2. Illustrative examples of cord lesions, which were matching or mismatching between sequences:
(A) Matched lesion between STIR and 3D T1 (located in the lateral column).
(B) Mismatched lesion, clearly visible on 3D T1, but hardly visible on STIR.
(C) Mismatched lesion with indefinite borders, clearly visible on STIR, but hardly visible on 3D T1.

Table 3. Total and median number of lesions detected by each rater on the different sequence combinations.

	STIR/ DE lesions	3D T1 lesions	Combined STIR/DE + 3D T1	p*	p**	p***
Rater 1 – total Rater 1 – median (range)	685 3 (0-12)	698 3 (0-10)	763 3 (0-12)	- 0.43	- 0.0004	- <0.001
Rater 2 – total Rater 2 – median (range)	717 3 (0-11)	708 3 (0-11)	746 3 (0-11)	- 0.43	- <0.001	- <0.001

*3D T1 *vs* STIR; **combined *vs* STIR; ***combined vs 3D T1

The results of mixed model analysis showed no difference in the mean number of lesions detected using STIR/DE alone and 3D T1 alone (p=0.83). Conversely, the number of lesions detected using the two sequences together was higher than compared with STIR/DE (p<0.001) and 3D T1 (p<0.001).

Figure 3. Distribution of cord lesions in the transverse section (A) and along the cranio-caudal axis (B) of the cervical cord.

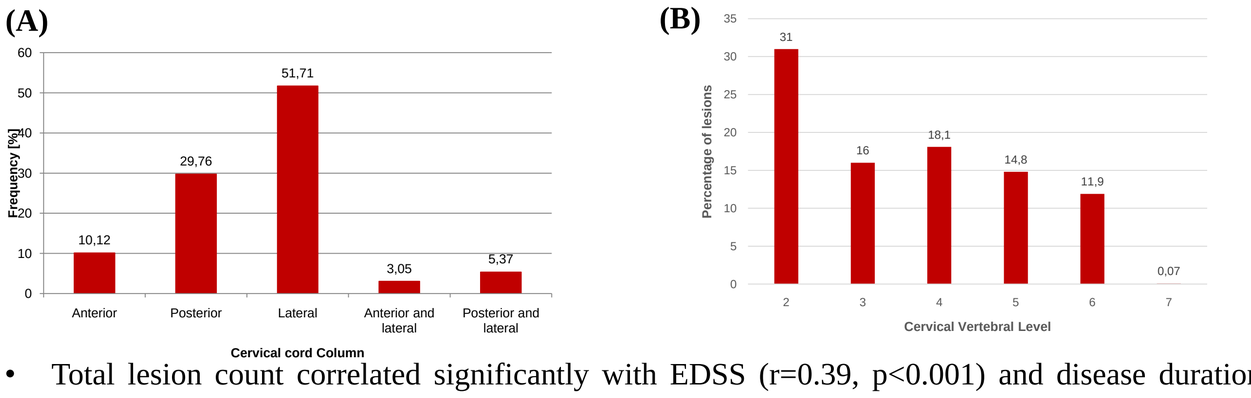

- Total lesion count correlated significantly with EDSS (r=0.39, p<0.001) and disease duration (r=0.44, p<0.001).
- The number of lesions located in the lateral, posterior and anterior columns correlated with clinical variables (highest correlation for lateral cord lesions: r=0.43 and 0.42, p<0.001).
- In RRMS, total cord lesions, lateral cord lesions and posterior cord lesions were correlated with EDSS and disease duration (EDSS: r=range 0.30-0.26, p=range 0.003-0.014, disease duration: r=range 0.39-0.37, p=range 0.001-0.002).
- In PPMS, trend toward a correlation between lesion counts and clinical variables (p=0.08).

CONCLUSIONS

- 3D T1 sequence at high field is sensitive in visualizing MS-related cord abnormalities, also in a multicenter context. Lesion detection on 3D T1 is reliable (high agreement between the two raters).
- When used in combination with conventional sequences (STIR/DE), the sagittal 3D T1 scan allows to detect a higher number of cord lesion and improves their localization.
- The improved ability of 3D T1 in localizing lesions in the transverse cord section might help diagnosis and might ameliorate correlations with disability.

REFERENCES

- Bot JCJ, Barkhof F, Lycklama AN, et al., *Radiology* (2002).
- Filippi M, Rocca M A, Ciccarelli O, et al., *The Lancet Neurology* (2016).
- Stroman PW, Wheeler-Kingshott C, Bacon M, et al., *NeuroImage* (2014).
- Nair G, Absinta M, Reich DS. *American Journal of Neuroradiology* (2013).

M. Aboulwafa has been supported by the ECTRIMS-MAGNIMS Fellowship in Magnetic Resonance Imaging. This study has been partially supported by a grant from FISM 2014/PMS/6.